Structural Complexity, Differential Response to Infection, and Tissue Specificity of Indolic and Phenylpropanoid Secondary Metabolism in Arabidopsis Roots[1[w]]

Paweł Bednarek*, Bernd Schneider, Aleš Svatoš, Neil J. Oldham[2], and Klaus Hahlbrock

Max Planck Institute for Plant Breeding Research, D–50829 Cologne, Germany (P.B., K.H.); and Max Planck Institute for Chemical Ecology, Beutenberg Campus, D–07745 Jena, Germany (B.S., A.S., N.J.O.)

Levels of indolic and phenylpropanoid secondary metabolites in Arabidopsis (*Arabidopsis thaliana*) leaves undergo rapid and drastic changes during pathogen defense, yet little is known about this process in roots. Using Arabidopsis wild-type and mutant root cultures as an experimental system, and the root-pathogenic oomycete, *Pythium sylvaticum*, for infections, we analyzed the aromatic metabolite profiles in soluble extracts from uninfected and infected roots, as well as from the surrounding medium. A total of 16 indolic, one heterocyclic, and three phenylpropanoid compounds were structurally identified by mass spectrometry and nuclear magnetic resonance analyses. Most of the indolics increased strongly upon infection, whereas the three phenylpropanoids decreased. Concomitant increases in both indolic and phenylpropanoid biosynthetic mRNAs suggested that phenylpropanoids other than those examined here in ''soluble extracts'' were coinduced with the indolics. These and previous results indicate that roots differ greatly from leaves with regard to the nature and relative abundance of all major soluble phenylpropanoid constituents. For indolics, by contrast, our data reveal far-reaching similarities between roots and leaves and, beyond this comparative aspect, provide an insight into this highly diversified yet underexplored metabolic realm. The data point to metabolic interconnections among the compounds identified and suggest a partial revision of the previously proposed camalexin pathway.

Pathogen defense in plants involves three types of antimicrobial secondary metabolite: preformed phytoanticipins, inducible phytoalexins, and infection-triggered breakdown products from preformed or newly induced, nontoxic precursors. Phytoanticipins and phytoalexins (VanEtten et al., 1994) can be subdivided into a variety of biosynthetically distinct classes (Mansfield, 2000; Dixon, 2001), whereas their breakdown products, as well as toxic breakdown products from other precursors, are chemically highly diverse. The chemical complexity of the plant defense response, including several different antimicrobial compounds that together comprise the biologically active toxic principle, renders this strategy robust in nature and all the more challenging for structural and functional dissection.

Comparison of Arabidopsis (*Arabidopsis thaliana*) leaves and roots is expected to provide further insight into the chemical nature and differentiated role of preformed and induced secondary metabolites in the pathogen defense of this species. Previous findings revealed an abundance of indolics among the infection-induced, aromatic compounds isolated with ''soluble extracts'' (operational definition) from Arabidopsis leaves, whereas the major phenylpropanoids either remained unaltered (flavonoids) or declined strongly (sinapoyl malate; Hagemeier et al., 2001). By contrast, phenylpropanoids as well as indolics were among the infection-induced cell wall-bound compounds in both leaves and roots (Hahlbrock et al., 2003; Tan et al., 2004). The most prominent soluble aromatic metabolites accumulating in Arabidopsis leaves during compatible or incompatible interactions with the bacterial pathogen, *Pseudomonas syringae* pv tomato, included Trp, β-D-glucopyranosyl indole-3-carboxylic acid, 6-hydroxyindole-3-carboxylic acid 6-*O*-β-D-glucopyranoside, and the phytoalexin camalexin (Hagemeier et al., 2001). A structurally unrelated, novel type of secondary metabolite, 3′-*O*-β-D-ribofuranosyl adenosine, was induced exclusively during compatible interactions (Bednarek et al., 2004).

These findings prompted further investigation of soluble extracts from Arabidopsis roots. Higher plant roots generally synthesize complex cocktails of biologically active secondary metabolites, several of which are produced exclusively in these underground organs (Flores et al., 1999). Roots further possess special means to modify the chemistry and, consequently, the biology of the surrounding rhizosphere by secreting root-specific, biologically active metabolites whose chemical nature and quantity depends on the nature and intensity of signals perceived from the environment (Flores et al., 1999; Walker et al., 2003a). Some of the secreted compounds are key players either in allelopathic

[1] This work was supported by the Fonds der chemischen Industrie.

[2] Present address: Dyson Perrins Laboratory, University of Oxford, Oxford OX1 2JD, UK.

* Corresponding author; e-mail bednarek@mpiz-koeln.mpg.de; fax 49–221–5062–315.

[w] The online version of this article contains Web-only data.

Article, publication date, and citation information can be found at www.plantphysiol.org/cgi/doi/10.1104/pp.104.057794.

interactions with other plants or in symbiotic or pathogenic interactions with microorganisms (Walker et al., 2003a; Bais et al., 2004).

In comparison to the numerous reports on Arabidopsis leaves (Hogge et al., 1988; Chapple et al., 1992; Veit and Pauli, 1999; Hagemeier et al., 2001; Bloor and Abrahams, 2002; Jones et al., 2003; von Roepenack-Lahaye et al., 2004), knowledge about both soluble, endogenous as well as secreted, and cell wall-bound (Tan et al., 2004) Arabidopsis root secondary metabolites is scarce. Notable exceptions are the occurrence of kaempferol and quercetin, mainly as aglycones, in roots from young seedlings (Peer et al., 2001); the constitutive presence of various indolic and aliphatic glucosinolates (Petersen et al., 2002; Brown et al., 2003); the further accumulation of some of these compounds in response to *Plasmodiophora brassicae* infections (Ludwig-Müller et al., 1999); and the accumulation of flavonoids, coniferin, and syringin in light-exposed roots (Hemm et al., 2004). Furthermore, constitutive secretion of various metabolites by agar grown roots (Narasimhan et al., 2003) and enhanced secretion of 3-indolepropanoic acid and of several benzoate and cinnamate derivatives into the root-surrounding liquid upon treatment with pathogen-derived elicitors or other signaling molecules have been reported (Walker et al., 2003b).

To complement a recent study on alkali-released, cell wall-associated indolic and phenylpropanoid compounds in Arabidopsis roots (Tan et al., 2004), we have focused here on the soluble counterparts, again with special emphasis on infection-induced changes, and with the aim of comparing aromatic secondary metabolism in leaves and roots as the two major vegetative organs. As readily accessible study objects, we used root cultures (Reintanz et al., 2001) and the oomycete, *Pythium sylvaticum*, for strong interactions with a pathogenic microorganism (van West et al., 2003). As several root secondary metabolites have important functions outside the plant, we analyzed not only endogenously accumulating, but also secreted, compounds. For methodological as well as comparative reasons, we confined our analyses again to the two major groups of UV-absorbing metabolite, phenylpropanoids and indolics (Hagemeier et al., 2001; Tan et al., 2004). Several mutants affected in the respective biosynthetic or signaling pathways served as tools for probing into the metabolic connections within each of the two groups.

RESULTS

Constitutively Occurring Aromatic Metabolites

Figure 1A shows a representative HPLC profile of soluble aromatic compounds in aqueous methanolic extracts from Arabidopsis root cultures grown under sterile conditions. One striking and obvious distinction from the corresponding profile of leaves (Chapple et al., 1992; Veit and Pauli, 1999; Hagemeier et al., 2001) was the apparent total absence of flavonol glycosides and sinapoyl esters, the most abundant soluble phenylpropanoids in Arabidopsis leaves. Conversely, root extracts contained three prominent phenylpropanoids that were not found in Arabidopsis leaves. These were identified by mass spectrometry (MS) and nuclear magnetic resonance (NMR) analyses (for all spectral data, see supplemental data) as coniferin (**1**), syringin (**2**), and scopolin (**3**; Figs. 1 and 2).

In contrast to this sharp distinction between roots and leaves at the level of soluble phenylpropanoid constituents, the indolic metabolite patterns were much more akin. Figure 2 shows the various indolic compounds (**4**–**17**, **19**, and **20**) that were unequivocally identified in roots or the root culture liquid (see also below). One of them, compound **9**, was initially isolated as a Lys conjugate (as determined by liquid chromatography [LC]/MS), but was unstable under the conditions used and decomposed to **9** during purification. The conjugate itself was not analyzed in further detail, due to both its low stability and the uncertainty whether it was a true natural product, rather than an artifact generated during extraction. However, the structure of the cleavage product, compound **9**, was verified by MS and ^{1}H NMR. One of the UV-absorbing compounds turned out to be neither phenylpropanoid nor indolic and was identified as 2-thioxo-1,3-thiazolidine-4-carboxylic acid (**18**). This compound was isolated previously from another crucifer, *Raphanus sativus*, and named raphanusamic acid (Hase et al., 1983).

In a modified experimental set up, we included an anion-exchange step in the purification procedure to increase the selectivity and sensitivity for the separation of acidic compounds. LC/MS analysis of the resulting purified samples confirmed the presence of free indole-3-carboxylic acid (**14**), whereas its 6-hydroxy counterpart could not be detected under the UV-analytical HPLC conditions used. During this analysis, we also identified a methyl derivative (**15**) of compound **14**, although the precise position of one additional, structurally verified methyl group could not be derived from the MS spectra with certainty.

Infection-Induced Changes

The unequivocally identified root constituents were analyzed for possible increases or decreases during infection with *P. sylvaticum* (Fig. 1B). Quantification of the respective HPLC data is presented in Figure 3, A to D. The two most prominent phenylpropanoids occurring in control roots, **1** and **2**, declined upon infection (Fig. 3A). Although a similar trend was observed for the third, somewhat less prominent phenylpropanoid (**3**), the results were in this case statistically not significant (Fig. 3B). By contrast, three of the four indolic metabolites, **4**, **7** (Fig. 3C), and **19**, which had previously been identified as major infection-induced compounds in Arabidopsis leaves infiltrated with *P. syringae* pv tomato (Hagemeier et al., 2001), were

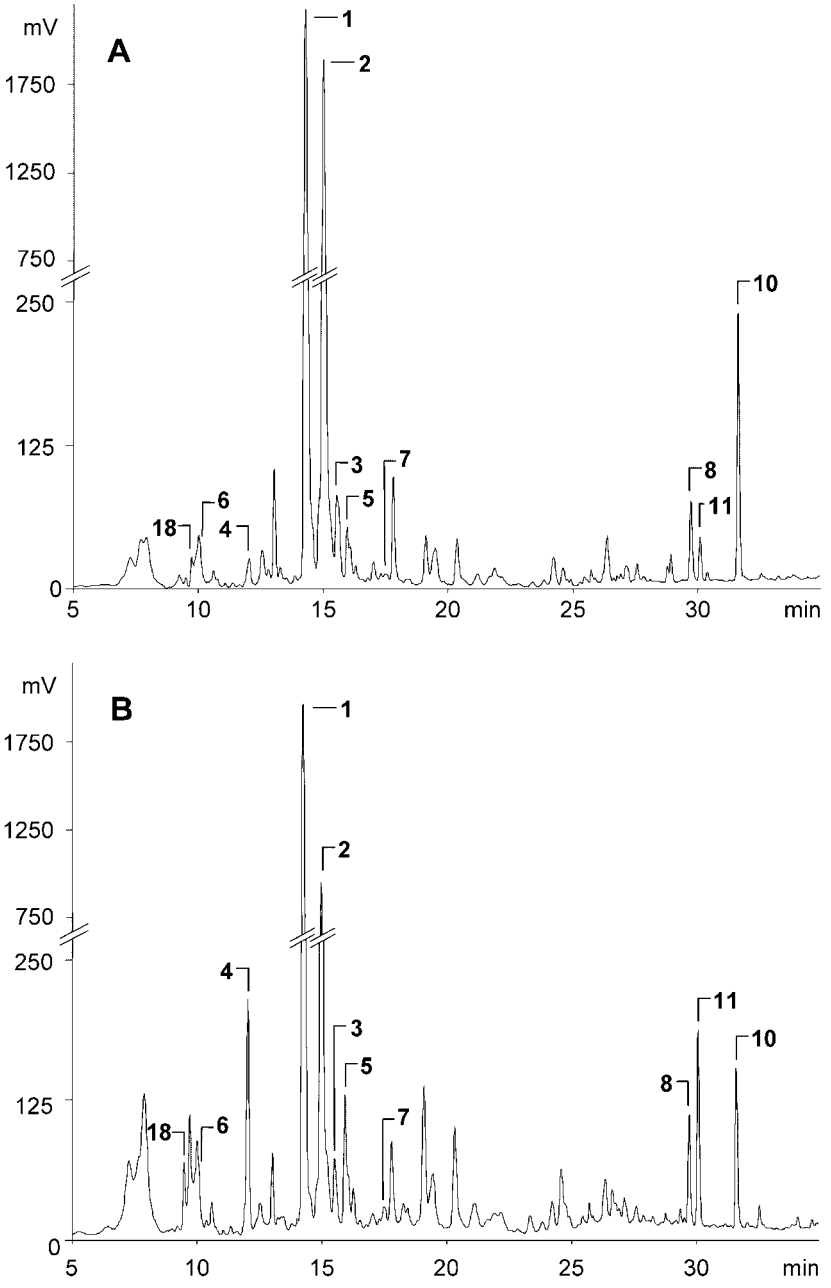

Figure 1. Comparison of soluble aromatic secondary metabolite profiles between uninfected and *P. sylvaticum*-infected Arabidopsis roots. A, HPLC profiles obtained with aqueous methanolic extracts from uninfected roots. B, Analogous profiles obtained from roots 48 h postinoculation with *P. sylvaticum*. For chemical structures of numbered compounds, see Figure 2.

likewise strongly induced in *P. sylvaticum*-infected roots. Of these three, compound **19**, the previously established phytoalexin in Arabidopsis, camalexin, was detectable only after infection (see below), again similar to the situation in leaves (Hagemeier et al., 2001). The fourth (one of the most strongly infection-induced compounds in Arabidopsis leaves, Trp) was too low in abundance to be accurately quantified in both uninfected and infected roots.

Compounds **5**, **14**, and **15** were also clearly induced during root infection (Fig. 3C). Interestingly, the apparent rate of induction was lower for the malonyl ester, **5**, than for the corresponding nonacylated, putative parent compound, **4**. Attempts to quantify the closely related glucosyl ester, **6**, and the single, nonaromatic compound analyzed, **18**, were unsuccessful. Both of them overlapped on chromatograms not only with one another, but also with additional, unidentified metabolites (Fig. 1). Higher separation efficiency would have been difficult to achieve without major alterations of the procedure used, as both **6** and **18** interacted very poorly with the RP-C18 column that otherwise was very efficient. The four methoxylated indole-3-carbaldehyde and indole-3-acetonitrile derivatives, **8** to **11**, displayed a differential induction behavior, in line with their substitution patterns; only the two 4-methoxy derivatives, **9** and **11**, were significantly induced upon infection (Fig. 3D).

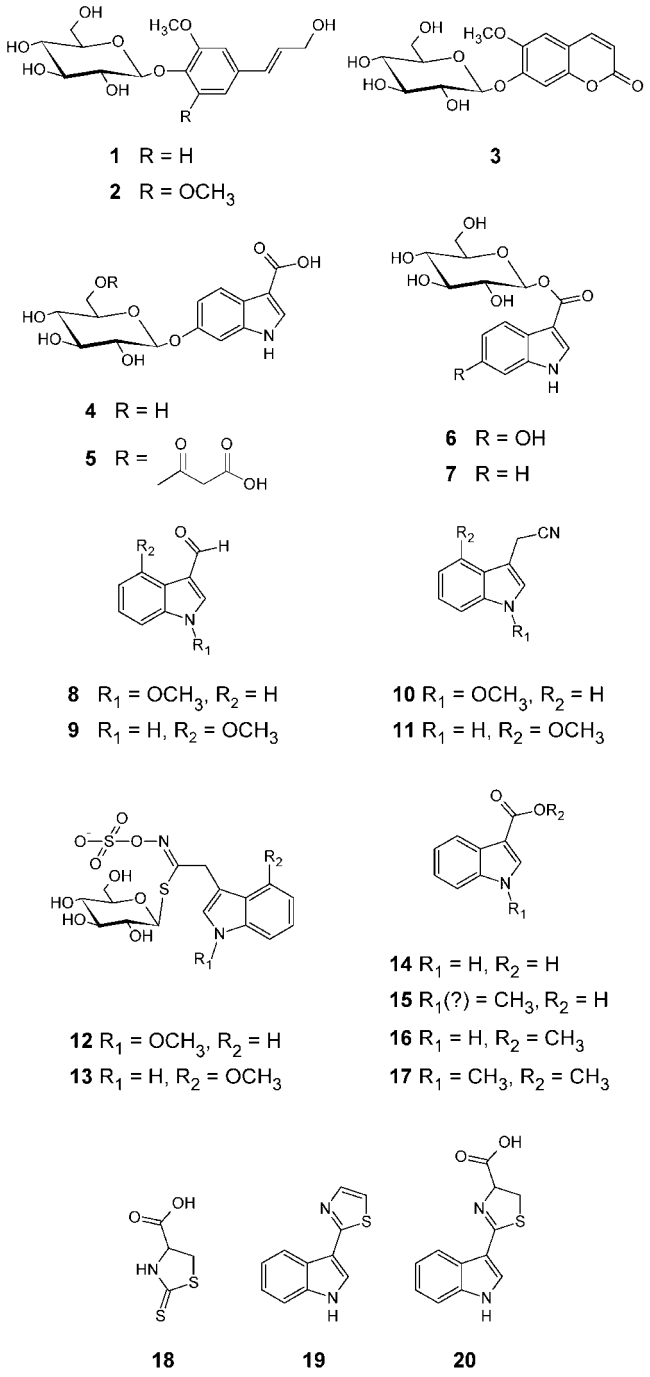

Figure 2. Chemical structures of all compounds identified in Arabidopsis roots. These are: **1**, coniferin; **2**, syringin; **3**, scopolin; **4**, 6-hydroxyindole-3-carboxylic acid 6-*O*-β-D-glucopyranoside; **5**, 6-hydroxyindole-3-carboxylic acid 6-*O*-(6′-malonyl)β-D-glucopyranoside; **6**, 6-hydroxyindole-3-carboxylic acid β-D-glucopyranosyl ester; **7**, indole-3-carboxylic acid β-D-glucopyranosyl ester; **8**, 1-methoxyindole-3-carbaldehyde; **9**, 4-methoxyindole-3-carbaldehyde; **10**, 1-methoxyindole-3-acetonitrile; **11**, 4-methoxyindole-3-acetonitrile; **12**, 1-methoxyindole glucosinolate; **13**, 4-methoxyindole glucosinolate; **14**, indole 3-carboxylic acid; **15**, methyl derivative of indole 3-carboxylic acid (undefined position); **16**, indole 3-carboxylic acid methyl ester; **17**, 1-methoxyindole 3-carboxylic acid methyl ester; **18**, 2-thioxo-1,3-thiazolidine-4-carboxylic acid; **19**, camalexin; **20**, 2-(indol-3-yl)-4,5-dihydro-1,3-thiazole-4-carboxylic acid.

To check if *P. sylvaticum* on its own can synthesize any of the induced compounds, samples prepared from oomycete tissue and its culture medium were analyzed by the same HPLC conditions as used for plant samples. None of the compounds identified in Arabidopsis samples was present in *P. sylvaticum* extracts (data not shown).

Indole Glucosinolates

Earlier reports on the degradation mode of indol-3-yl glucosinolate in vitro (Bradfield and Bjeldanes, 1987a; Latxague et al., 1991) had suggested that compounds **8** to **11** could be break-down products of **12** and **13**, the two major, constitutively occurring glucosinolates in

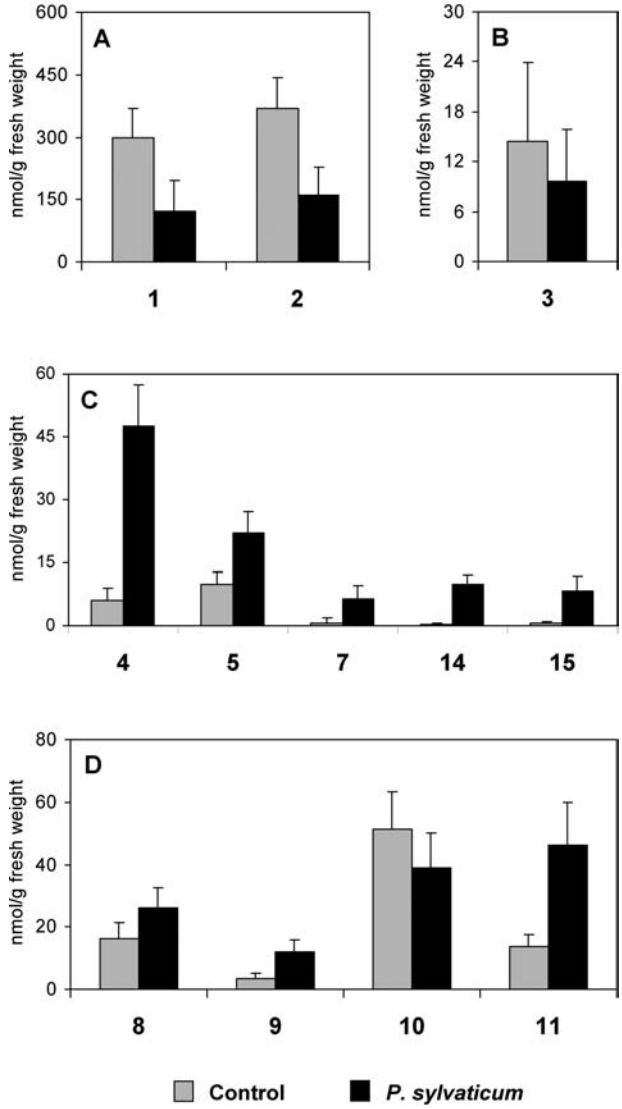

Figure 3. Comparison of metabolite levels in uninfected controls and Arabidopsis roots 48 h postinoculation with *P. sylvaticum*. A, Monolignol glucosides. B, Scopoletin. C, Members of the indole-3-carboxylate class. D, Glucosinolate break-down products. Bars indicate SD from at least five independent measurements.

Arabidopsis roots (Petersen et al., 2002; Brown et al., 2003). To test this possibility in our context, we changed the isolation procedure by using freeze-dried tissue and boiling aqueous methanol for extraction to prevent glucosinolate degradation during these first two critical steps. The glucosinolates were then indirectly verified by eluting the corresponding desulfoglucosinolates with sulfatase from an anion-exchange column (Thies, 1979). Under these conditions, the relative abundance of compounds **8** to **11** in the original extracts, as compared with trace amounts of the desulfoglucosinolates (representing the glucosinolates), was reversed to the opposite relationship. Quantitative estimation of the results (Fig. 4) demonstrated that sizable amounts of the two indole glucosinolates, **12** and **13**, were constitutively present in roots, but were largely degraded to **8** to **11** if extracted from fresh-frozen tissue at room temperature.

Mutant Analysis

Four Trp-biosynthetic mutants, *trp1-100*, *trp2-100*, *trp3-1*, and *trp5-1* (Radwanski and Last, 1995), and four mutants affected in three major, defense-related signaling pathways, *NahG*, *pad4-1*, *ein2-1*, and *jar1-10* (Glazebrook, 2001), were used to test for possible effects on the presence and induction behavior of the various compounds analyzed. Similar to the results reported in earlier studies (Zhao and Last, 1996; Brader et al., 2001), none of the four *trp* mutants differed significantly in either regard from the corresponding wild-type plants, whether infected or uninfected. The only differences observed were the accumulation of anthranilate glucoside in *trp1-100* roots and increased levels of Trp in *trp5-1* roots, again analogous to similar findings with leaves from the same two mutants (Radwanski and Last, 1995).

Of all eight mutants tested, only *NahG* and *jar1-10* showed one or two significant differences each from wild type regarding the various compounds analyzed here. In *NahG* roots, camalexin (**19**) accumulated to considerably lower levels during infection than observed with wild-type roots (see below), similar to the situation reported for leaves (Zhao and Last, 1996), and *jar1-10* contained greatly reduced levels of compound **2** in uninfected roots, and increased levels of **9** and **11** upon infection. Figure 5 shows that the induction rates of **9** and **11** corresponded well with the induction rate observed for the corresponding desulfoglucosinolate, **D-13**, under the appropriately modified extraction conditions (Fig. 4).

Secreted Compounds

As considerable amounts of root secondary metabolites occur in the rhizosphere, we further analyzed the culture liquid of uninfected and infected roots for the presence of indolic and phenylpropanoid compounds. Similar to the results obtained above with root extracts, the metabolite profiles in the culture medium were strongly affected by *P. sylvaticum* infections. Most or all of the infection-induced compounds, with the

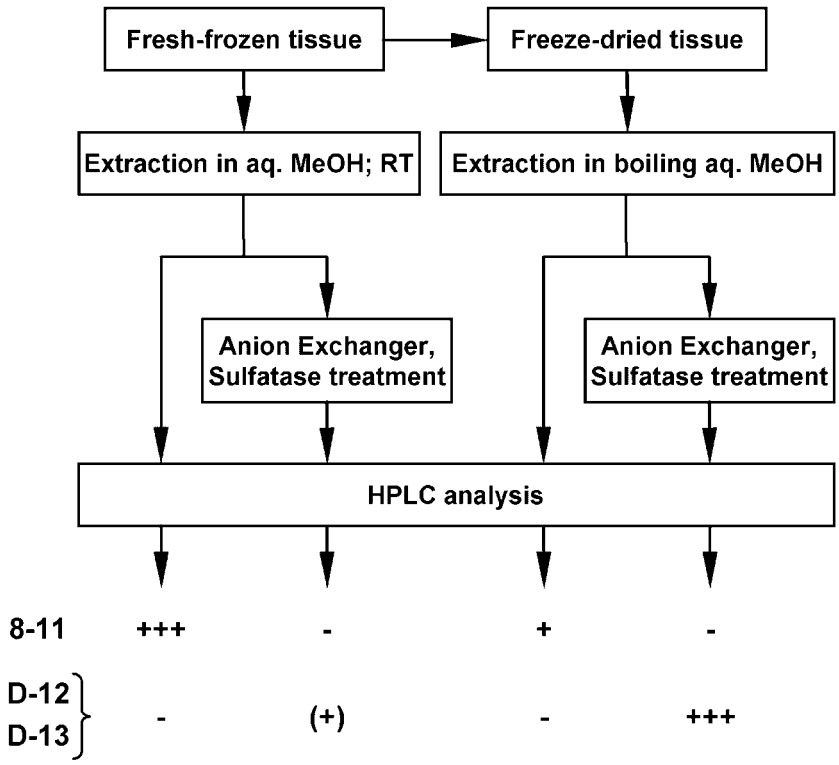

Figure 4. Outline of the extraction procedures preferentially yielding either glucosinolate degradation products (left) or desulfoglucosinolates (right). Estimated relative amounts of degradation products (sum of **8–11**) and desulfoglucosinolates (sum of desulfo-**12** [**D-12**] and desulfo-**13** [**D-13**]) recovered from the respective HPLC columns are indicated by the number of + symbols. The − symbols indicate inappropriate isolation conditions for the respective compounds.

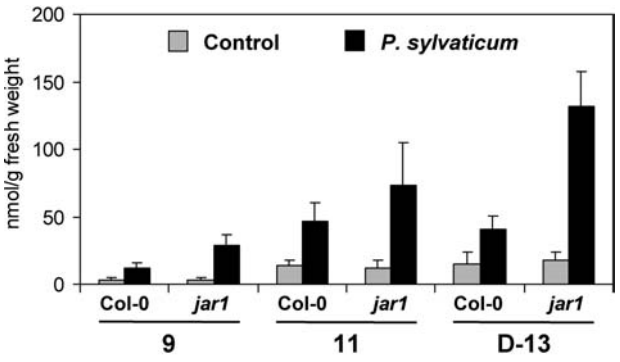

Figure 5. Comparison of metabolite levels in uninfected and infected wild-type (Col-0) and mutant (*jar1-10*) Arabidopsis roots 48 h postinoculation with *P. sylvaticum*. Bars indicate SD from at least five independent measurements.

possible exception of **8** to **11**, occurred both within roots (see above) and in the surrounding liquid. Three of them, **16**, **17**, and **20**, which were subsequently also detected within roots under appropriately modified conditions (see below), were sufficiently abundant for structural analysis. In fact, **16** and **17** were the two most abundant peaks on HPLC chromatograms obtained from the liquid of uninfected roots and accumulated strongly upon infection (Fig. 6). They were identified as indole-3-carboxylic acid methyl ester (**16**) and its 1-methyl derivative (**17**).

The other strongly infection-induced metabolite that had not been detected within roots, compound **20**, was very prominent in the liquid after infection, but undetectable in the untreated control. In agreement with a UV spectrum closely resembling that of camalexin (**19**), **20** was identified as 2-(indol-3-yl)-4,5-dihydro-1,3-thiazole-4-carboxylic acid (Fig. 2), a previously proposed intermediate in camalexin biosynthesis (Zook and Hammerschmidt, 1997), which, however, had not been detected in Arabidopsis. The structural identity of **20** was further verified by comparing its spectral properties with those of the authentic compound that had been synthesized from indol-3-ylacetonitrile and L-Cys (A. Svatos and J. Sproß, unpublished data). Consequential reexamination of root extracts by LC/MS analysis revealed the presence of **20** in infected roots as well. To exclude the possibility that this compound is a *P. sylvaticum*-specific product of camalexin detoxification or of another kind of modification, we performed an analogous experiment using extracts from Arabidopsis leaves that had been infiltrated with an avirulent strain of *P. syringae* pv tomato (Hagemeier et al., 2001). Indeed, LC/MS analysis verified **20** in these extracts as well.

To further probe into the possible metabolic relationship between **19** and **20**, their accumulation behavior was monitored in roots and in the culture liquid of infected *NahG*, *pad3-1*, *pad4-1*, and *pad5-1* mutants (Fig. 7). *Pad3-1* and *pad5-1* are thought to be camalexin-biosynthetic mutants (Glazebrook and Ausubel, 1994; Glazebrook et al., 1997; Zhou et al., 1999), whereas *pad4-1* and *NahG* are suspected to be affected in the signaling involved in camalexin accumulation (Glazebrook, 2001). At 48 h postinoculation of roots with *P. sylvaticum*, the induced amounts of both **19** and **20** were lower in *pad4-1* and *NahG* than in wild-type (Columbia [Col-0]) roots or root culture liquid. By contrast, in the culture liquid of infected *pad3-1* and *pad5-1* roots, **20** accumulated to higher levels than observed with the wild-type control, whereas both mutants accumulated and secreted **19** at levels even below those reached in *pad4-1* or *NahG* roots.

Infection-Induced Changes in mRNA Amounts

To see whether the observed infection-induced changes in indolic and phenylpropanoid metabolite levels correlated with changes in the amounts of the respective biosynthetic mRNAs, total RNA was prepared from the same tissue samples as used above for secondary product identification. Samples were taken at different time points from uninfected and *P. sylvaticum*-infected wild-type Arabidopsis roots, as well as from *P. sylvaticum*-infected *jar1-10* roots, and were analyzed by blot hybridization. The *jar1-10* mutant was included in this analysis because of its increased susceptibility to *P. sylvaticum* as compared with the wild type (Staswick et al., 1998; Vijayan et al., 1998). The DNA probes used were specific for mRNAs encoding the following enzymes: anthranilate synthase α-subunit 1 (ASA1); Trp synthase α-subunit (TSA); Trp synthase β-subunit (TSB; Radwanski and Last, 1995); and three putative P450 monooxygenases, CYP79B2, CYP79B3 and CYP83B1 (Wittstock and Halkier, 2002), all representing indolic biosynthetic pathways; and Phe ammonia-lyase (PAL; Wanner et al., 1995), cinnamate 4-hydroxylase (C4H; Bell-Lelong et al., 1997), and cinnamoyl-CoA reductase 2 (CCR2; Lauvergeat et al., 2001) from phenylpropanoid biosynthesis.

All tested mRNAs were strongly induced by root infection, with the possible exception of CYP79B3 that was too low in abundance to give clearly identifiable signals (Fig. 8). Conversely, CYP83B1 increased, but

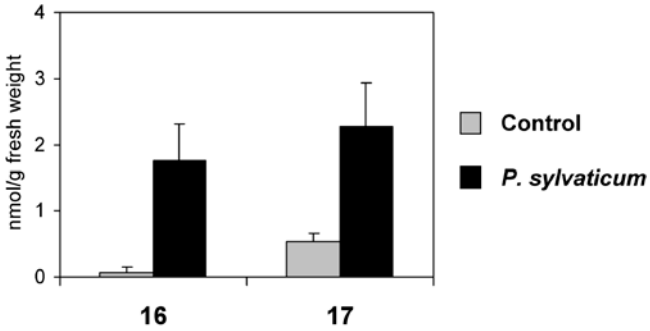

Figure 6. Comparison of indolic methyl ester levels in the culture liquid from uninfected controls and Arabidopsis roots 48 h postinoculation with *P. sylvaticum*. Bars indicate SD from at least five independent measurements.

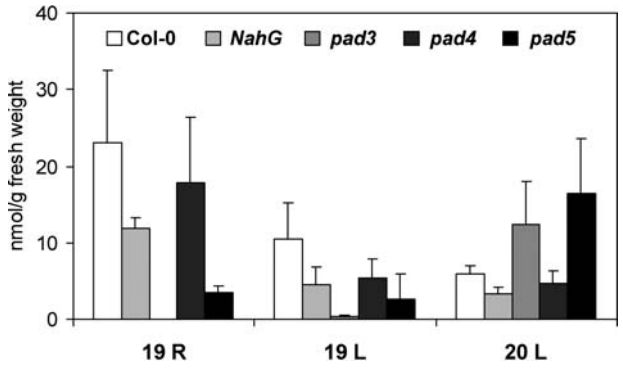

Figure 7. Comparison of metabolite levels in infected wild-type (Col-0) and mutant Arabidopsis roots (R) and root culture liquid (L) 48 h postinoculation with *P. sylvaticum*. Bars indicate SD from at least five independent measurements.

the background level was too high to precisely estimate the extent of induction. These two extreme cases were not further pursued, as the common trend was clearly evident from all other mRNAs studied. In wild-type roots, the mRNAs increased abruptly after a lag period of about 8 to 12 h postinoculation, probably indicating the length of the preinfection time required for fungal development from cultured mycelium to the actual infectious agent. Following this sudden increase, the mRNA levels remained high for at least 24 h and then appeared to decline slowly. As the precise timing of the initial increases was not determined, it remains open whether or not the apparent difference between the time courses of induction for PAL and C4H mRNAs on the one hand and all others on the other hand is real. However, a very clear-cut result was a delay of mRNA induction in *jar1-10* roots as compared with the wild-type control (Fig. 8).

Effects of Growth Conditions on Secondary Metabolism

In all of these experiments, the root cultures were routinely grown under a 12-h-light/-dark regime using dim white light at 15 to 20 μE m^{-2} s^{-1}. To see whether this low dosage of intermittent light had any effects on phenylpropanoid metabolism, we also analyzed roots grown in total darkness. Recently, Hemm et al. (2004) reported the induction of compounds **1** and **2**, along with flavonol glycosides, upon illumination of Arabidopsis roots using either continuous light or 16-h-light periods, both at 100 μE m^{-2} s^{-1}. Under our conditions, there was no significant difference in the levels of **1** (approximately 300 μg/g fresh weight [fw]), **2** (approximately 350 μg/g fw), and flavonol glycosides (not detectable by HPLC/UV) between light- and dark-grown roots. However, direct comparison of these data with those of Hemm et al. (2004) is impaired by marked differences not only in light intensity (see above), but also in root age (4 versus 2 weeks) and propagation method (liquid culture versus agar plates).

Analyses of samples prepared from leaves of liquid-grown seedlings (data not shown) revealed a typical Arabidopsis leaf profile of secondary metabolites with derivatives of flavonols and of sinapic acid as the major phenolic compounds (Chapple et al., 1992; Jones et al., 2003).

DISCUSSION

Aromatic Secondary Metabolism in Arabidopsis Roots and Leaves

These results and previous findings allow us to draw three general conclusions: (1) Arabidopsis roots and leaves differ greatly with regard to all major, soluble phenylpropanoid constituents; (2) by sharp contrast, indolic metabolism, though similarly complex, is remarkably uniform between roots and leaves; (3) in both organs, pathogen defense is associated with decreases in soluble phenylpropanoids and increases in soluble indolics.

The strictly organ-specific occurrence of soluble phenylpropanoids extends to all secondary metabolites observed so far in Arabidopsis (Chapple et al., 1992; Veit and Pauli, 1999; Hagemeier et al., 2001; Bloor and Abrahams, 2002; Jones et al., 2003), with the conditional exception that flavonol glycosides, which are absent in dark-grown roots, are induced by sufficiently high doses of light not only in leaves (Li et al., 1993), but also in roots (Hemm et al., 2004). The most characteristic, highly predominant soluble phenylpropanoids in roots are the two monolignol glucosides (**1** and **2**) and the coumarin derivative, scopolin (**3**). Despite a thorough search by LC/MS, we were unable

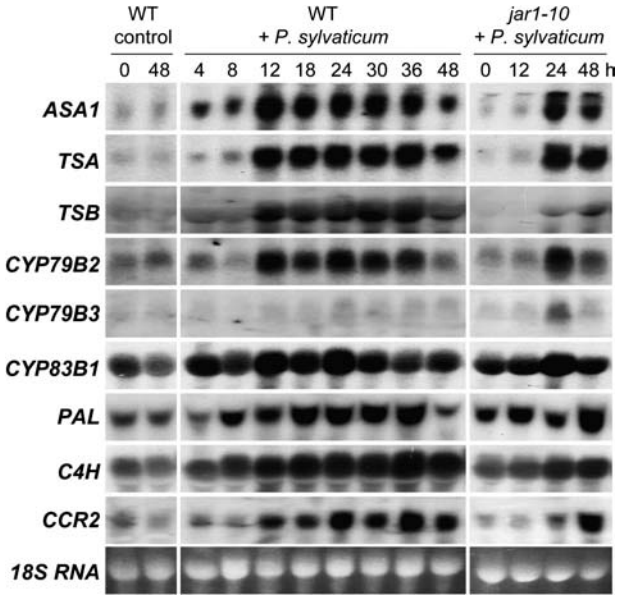

Figure 8. Induction of indolic and phenylpropanoid biosynthetic mRNAs upon Arabidopsis root infection with *P. sylvaticum*. RNA isolated from roots at the indicated times postinoculation was blotted onto polyacrylamide gels and probed with the indicated cDNAs (see text for further explanation).

to detect any one of these three root constituents in Arabidopsis leaves. This mutually exclusive occurrence of phenylpropanoid metabolites in roots and leaves is not restricted to Arabidopsis and has been reported for other plant species as well (Bednarek et al., 2001; Bennett et al., 2003). Remarkably, the sharp distinction between roots and leaves at the level of soluble phenylpropanoid constituents does not apply to their cell wall-bound counterparts. In a recent, analogous study on alkali-released cell wall constituents, phenylpropanoids not only exhibited almost identical metabolite profiles in Arabidopsis roots and leaves, but were also induced in a similar manner upon pathogen infection in both organs (Tan et al., 2004).

In contrast to the phenylpropanoids, the indolic patterns in soluble Arabidopsis root and leaf extracts were very similar, perhaps even identical at the current level of resolution. However, despite the identification of several new indolic metabolites, and despite the existence of numerous detailed studies on the biosynthesis of indolic glucosinolates and indole-3-acetic acid (IAA) in Arabidopsis leaves (Ljung et al., 2002; Wittstock and Halkier, 2002), it is still difficult to estimate the full extent to which indolic metabolism overlaps in roots and leaves. Obvious reasons for this are the unknown degree of structural diversity of the individual compounds, the large developmental and organ-specific fluctuations in their relative abundance, and the paucity of direct and detailed comparative studies. For example, of the 17 indolic (**4**–**17**, **19**, and **20**) or structurally related (**18**) compounds identified here, no more than two (**12** and **13**) had been observed before in both Arabidopsis roots and leaves (Hogge et al., 1988; Ludwig-Müller et al., 1999); three (**4**, **7**, and **19**) in Arabidopsis leaves only (Tsuji et al., 1992; Hagemeier et al., 2001); and four others (**5**, **6**, **16**, and **20**) are novel plant constituents that, to the best of our knowledge, have not been reported for any plant species. The remaining ones (**8**–**11**, **17**, and **18**) have previously been reported from other cruciferous species (Nomoto and Tamura, 1970; Hase et al., 1983; Wakabayashi et al., 1986; Bradfield and Bjeldanes, 1987b; Conn et al., 1994; Pedras et al., 2003), but not from Arabidopsis.

Monolignols and Scopolin: Putative Preformed, Defense-Related Compounds

The biological functions of monolignol 4-*O*-β-D-glucosides, including compounds **1** and **2**, and of the various coumarins, such as compound **3**, have not been defined with certainty. Monolignol glucosides are typical constituents of gymnosperms, but have also been reported to occur in some angiosperms, including Arabidopsis (Boerjan et al., 2003; Hemm et al., 2004). These compounds have been postulated to act as storage and/or transport forms of lignin precursors (Whetten and Sederoff, 1995), but unequivocal evidence for this role is still lacking (Boerjan et al., 2003).

The decline of **1** and **2**, and probably **3**, during root infection from previously high constitutive levels suggests functions of these three compounds in pathogen defense different from those of the induced soluble indolics. A plausible explanation for the decline of **1** to **3** during infection would be a role as preformed, rapidly mobilized precursors of more or less immediately defense-related compounds. Likely products would be lignin or lignin-like barrier substances (from **1** and **2**) and the phytoalexin, scopoletin (from **3**), which could act as a broad-range antibiotic agent (Harborne, 1999). Additionally, or alternatively, scopoletin, an efficient peroxidase substrate in vitro (Marquez and Dunford, 1995), may act in vivo as scavenger of reactive oxygen species and thus prevent, or reduce, oxidative damage in infected or otherwise stressed plant cells (Chong et al., 2002). Such a role of **3** in plant defense would be in line with the observation that glucosylation of scopoletin and the consequential accumulation of scopoletin 4-*O*-glucoside (**3**) are crucial for the defense of *Nicotiana tabacum* against tobacco mosaic virus (Chong et al., 2002).

In any event, the observed induction of phenylpropanoid biosynthetic mRNAs would not contradict the decline of phenylpropanoids in the soluble fraction, but is most probably related to the concomitant accumulation of phenylpropanoids at specific defense-related sites, including increased turnover rates in the compartments analyzed.

Classification, Inferred Metabolic Relationships, and Possible Functions of Indolic Secondary Metabolites

In contrast to all major, soluble phenylpropanoids, numerous indolics were induced and none was significantly repressed upon infection. The lack of detectable Trp induction in infected roots, despite the strong up-regulation of several Trp biosynthetic mRNAs, might point to an increased turnover rate of Trp, in accord with its precursor function for at least some of the accumulating indolics. Remarkably, our experiments using *trp* mutants indicated that altered rates of Trp biosynthesis had no significant effects on the levels of any of the indolics analyzed, in full agreement with similar data on the camalexin (Zhao and Last, 1996) and indole glucosinolate (Müller and Weiler, 2000; Brader et al., 2001) levels in infected Arabidopsis leaves. Although these results are surprising in view of the Trp dependence of glucosinolate and camalexin formation (Wittstock and Halkier, 2002; Glawischnig et al., 2004), we note that the *trp* mutants analyzed here were still able to synthesize some Trp (Radwanski and Last, 1995). The remaining pool may suffice for unimpaired glucosinolate and camalexin production, particularly if Trp is not involved in the formation of most of the other indolics.

The occurrence of numerous indolic metabolites in the root culture liquid or rhizosphere raises a number of questions concerning their biological functions. Are they specifically synthesized and actively secreted, or

do they stem from passive leakage of damaged tissue or from a combination of both? The relatively large abundance of some indolics, such as camalexin, **20**, and, even more so, the two methyl esters, **16** and **17**, in the culture liquid, as compared with root extracts, might indicate the existence of active secretion mechanisms.

Using the class-defining type of substitution in the 3-position of the indole ring for subdivision of all of indolics discussed here from Arabidopsis, the following classes can be distinguished: (1) indole-3-carboxylate and its derivatives; (2) indole glucosinolates and their degradation products; and (3) camalexin and related compounds. Additional ring substitutions besides the class-defining primary substitutions in the 3-position will be designated in the following as secondary.

The first class comprises the various indole-3-carboxylate derivatives, including **4** to **7**, **14** to **17**, and the cell wall conjugate of **14** (Hagemeier et al., 2001; Tan et al., 2004). As secondary ring substitutions other than partial 6-hydroxylation have not been observed among the various Glc and cell wall conjugates, and conversely, no hydroxyl but only methyl substitutions were detected among the free acids and methyl esters, the overall size of this class may be considerably larger than observed so far. Three likely reasons for the possibly low number of detected members are immediately apparent: (1) the HPLC profiles obtained with soluble aromatic metabolites contained numerous relatively minor, as yet unidentified compounds (Fig. 1); (2) *N*-methylation (as in **15** and **17**), if also occurring in cell wall conjugates, might have been lost during the alkali treatment used for cleavage from cell walls (Tan et al., 2004); and (3), considering the lability of the malonyl ester bond (Kreuzaler and Hahlbrock, 1973, Bednarek et al., 2001), the actual degree of malonylation of Glc conjugates in vivo may be higher than detected under the present conditions in vitro. Although the functions of the various class members are unknown, the strong induction of most of them in response to pathogen infection suggests a major role in disease resistance. In particular, the remarkably high accumulation rate of indole-3-carboxylate in the cell wall during infection seems to indicate an important function in this compartment (Tan et al., 2004).

Whether the methyl esters, **16** and **17**, are true natural products or were artificially generated through transesterification in the course of the isolation procedure remains to be clarified. However, it may be of interest in this connection to note that Zubieta et al. (2003) identified a methyltransferase from Arabidopsis capable of catalyzing in vitro formation of IAA methyl ester, a close structural analog of compounds **16** and **17**.

The second class, the indolic glucosinolates and their degradation products, displays great chemical complexity. The unequivocal definition of this class through the glucosinolate residue of the parent compounds, combined with the verification of the correspondingly substituted indole-3-acetonitriles and indole-3-carbaldehydes as their break-down products, clearly demands that at least these three structural variants (exemplified by compounds **8**–**13** in Fig. 2) together constitute this class of indolics. Although the unsubstituted and the 4-hydroxylated indole glucosinolates have been shown to occur in roots, though in smaller amounts than the 1- and 4-methoxylated ones (Petersen et al., 2002; Brown et al., 2003), neither these nor the corresponding break-down products were detected in our analyses. This negative coincidence further supports the notion of a close metabolic relationship among the respective substitution types of glucosinolates, acetonitriles and free aldehydes. Notably, previously reported degradation of indole glucosinolates to 3,3′-diindolylmethane (Bradfield and Bjeldanes, 1987a; Latxague et al., 1991) was not observed in this study.

In Arabidopsis leaves, the constitutively present, unsubstituted indole glucosinolate was shown to be further induced more strongly than its 4-methoxy derivative by treatment with elicitor (Brader et al., 2001). Endogenous, defense-related signal molecules can also act as indole glucosinolate-inducing agents (Mikkelsen et al., 2003). Our present data indicate that in roots only one of the two methoxylated glucosinolates (**13**) increases during *P. sylvaticum* infection. In fact, the other one (**12**), together with its break-down products (**10** and **11**), was the only indolic metabolite identified in this study that did not significantly increase during infection. Whatever the reason, distinct 1- and 4-*O*-methyltransferase activities may, at least in part, be responsible for different rates of synthesis of the methoxylated indole glucosinolates (Mikkelsen et al., 2003).

Mikkelsen et al. (2003) concluded from their data that the induction of **13** in Arabidopsis leaves involves the salicylate and ethylene, but not the jasmonate, signaling pathways. According to our present results using Arabidopsis mutants defective in the respective pathways, the infection-induced accumulation of **13** in roots remained largely unaffected in the salicylate (*NahG* and *pad4-1*) and ethylene (*ein2-1*) signaling mutants, but was strongly enhanced in the jasmonate (*jar1-10*) signaling mutant. According to Brader et al. (2001), the induction in leaves of unsubstituted indole glucosinolate is abolished in a different type of mutant defective in the jasmonate pathway (*coi1-1*). However, it should be noted that although JAR1 and COI1 are supposed to be closely linked in the jasmonate signaling pathway (Glazebrook, 2001), infection phenotypes of *jar1* and *coi1* mutants can differ drastically (Kloek et al., 2001).

The third, camalexin class of indolics appears so far to be more narrowly confined to camalexin itself (**19**) and its carboxy derivative (**20**). The accumulation of camalexin in infected Arabidopsis leaves (Tsuji et al., 1992; Thomma et al., 1999) and its antimicrobial properties in vitro (Rogers et al., 1996) have been amply demonstrated. An essential role

in pathogen defense was not always apparent (Glazebrook and Ausubel, 1994; Glazebrook et al., 1997), but could be verified, e.g. for *Alternaria brassicicola* infections of Arabidopsis leaves (Thomma et al., 1999). Our present data indicate that camalexin could have a similar function in roots, including the rhizosphere. Consistent with this view, we have shown that camalexin induction in infected roots is impaired by the *pad3-1*, *pad4-1*, *pad5-1*, and *NahG* mutations in a similar manner as reported for leaves (Glazebrook and Ausubel, 1994; Zhao and Last, 1996; Glazebrook et al., 1997).

An important finding was the identification of raphanusamic acid (**18**) along with **19** and **20**, which renders **18** a highly probable intermediate in the biosynthesis of camalexin and suggests a revision of the previously assumed camalexin pathway (Fig. 9). Our data indicate that **18**, a readily conceivable derivative of Cys (Zook and Hammerschmidt, 1997), is constitutively present in roots and thus immediately available for camalexin synthesis upon infection. Furthermore, increased accumulation of **20** was observed in the root culture liquid of both the *pad3-1* and *pad5-1* camalexin-deficient mutants. This finding not only supports the notion that **20** is a precursor of camalexin (Zook and Hammerschmidt, 1997), but also suggests a relocation of PAD3 within the camalexin pathway. Rather than confirming the previous assignment of PAD3 to an early step in the pathway (Zhou et al., 1999), our data indicate a late position close to PAD5, that is, between **20** and **19** (Fig. 9). As PAD3 is a P450 monooxygenase (Zhou et al., 1999), a plausible mechanism would be the formation of **19** from **20**, probably in this order, through hydroxylation, decarboxylation, and dehydration of the heterocyclic ring to yield camalexin as the metabolic end product.

CONCLUSIONS AND OUTLOOK

Together, this and the three preceding, complementary studies (Hagemeier et al., 2001; Bednarek et al., 2004; Tan et al., 2004) have identified most or all of the major, readily accessible aromatic metabolites occurring in untreated and variously infected Arabidopsis Col-0 plants. The combined results revealed a strikingly differential behavior of indolic and phenylpropanoid metabolism regarding tissue specificity, defense response, and accumulation in the soluble and cell wall compartments. The example of IAA indicates that at least one, possibly more, functionally important, low-abundance metabolites have remained undetected, suggesting that the overall structural diversity in vivo is even greater than hitherto uncovered. Another important, largely unexplored phenomenon is the regulatory interplay between different metabolic realms, e.g. as recently reported for glucosinolate and phenylpropanoid metabolism (Hemm et al., 2003) and for functionally distinct phenylpropanoid pathways (Logemann and Hahlbrock, 2002). Furthermore, refined analyses at the level of individual cells or cell types will undoubtedly reveal yet another layer of spatial, metabolic, and functional complexity.

Concerning the role of indolic and phenylpropanoid secondary metabolism in pathogen defense, the now existing overview of the constitutive and induced or repressed levels of major representatives will serve as a guideline for more specifically targeted studies on

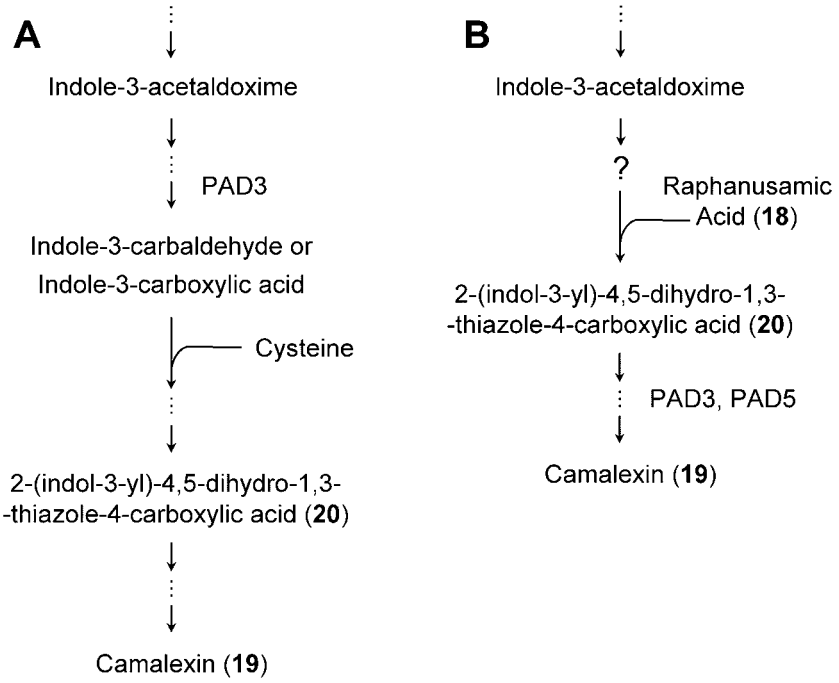

Figure 9. Comparison of previously and newly proposed camalexin pathways. A, Pathway combining proposals of Zook and Hammerschmidt (1997); Zhou et al. (1999); and Glawischnig et al. (2004). B, Alternative pathway proposed on the basis of results of this article.

the functional significance of individual metabolites, subclasses or classes. However, similar to the partially opposing findings with camalexin (see above), the results will probably differ markedly between pathosystems and ecotypes. As pathogen defense in plants consists of a highly complex, multi-component strategy involving a plethora of physical and chemical means, including variable blends of toxic agents, each pathogen has evolved its own attempts to overcome the plants' defense measures. Therefore, the path of detailed functional assignments may be long, but the road seems to be paved.

MATERIALS AND METHODS

Plant Material

Seeds of Arabidopsis (*Arabidopsis thaliana*) ecotype Col-0 were from Lehle Seeds (Round Rock, TX). Seeds of *ein2-1*, *jar1-10*, *pad4-1*, *pad3-1*, *pad5-1*, *trp1-100*, *trp2-100*, *trp3-1*, and *trp5-1* mutants were obtained from the Nottingham Arabidopsis Stock Center (Loughborough, UK). Seeds of *NahG* plants were a kind gift of Dr. Volker Lipka (University of Tübingen, Germany). Liquid cultures of Arabidopsis were established, with minor modifications, as described by Reintanz et al. (2001) and were grown for 4 weeks at 20°C under a 12-h low-intensity white-light regime (15–20 μE m^{-2} s^{-1}).

Infections

Pythium sylvaticum strain DSM 2322 (Deutsche Sammlung von Mikroorganismen und Zellkulturen, Braunschweig, Germany) was grown for 1 week on potato dextrose agar plates (Becton-Dickinson Microbiology Systems, Sparks). A single piece of agar (approximately 2 × 2 mm) with mycelium was transferred to the root culture medium. After 48 h, infected and control roots (approximately 0.5 g each) were harvested, frozen in liquid N_2, and stored at −80°C. The culture liquid was filtrated and stored at −20°C. *Pseudomonas syringae* pv tomato, strain DC3000 carrying the avirulence gene *avrRpm1*, was grown and infiltrated into Arabidopsis leaves as described by Hagemeier et al. (2001). Leaf samples (approximately 0.2 g) were collected 48 h postinoculation, frozen in liquid N_2, and stored at −80°C.

Extraction Procedure and HPLC Analysis

After addition of 70% (roots) or 50% (leaves) aqueous methanol (v/v; 0.6 mL each), the tissue was homogenized using zirconia beads (1 mm; Roth, Karlsruhe, Germany) in a Mini-Beadbeater-8 (Biospec Products, Bartlesville, OK) and centrifuged for 15 min at 20,000*g*. The pellets were reextracted with 0.6 mL methanol, centrifuged again, and supernatants were combined where appropriate. The solvent was removed at 30°C using a Speed-Vac (Eppendorf, Hamburg, Germany) and the residue was redissolved in 80% aqueous methanol (1 μL/5 mg initial fresh weight). Phenolic acids were isolated from root extracts corresponding to approximately 2 g of fresh tissue using Supelclean LC-SAX SPE cartridges (500 mg; Supelco, Bellefonte, PA) according to the protocol described by Głowniak et al. (1996). Collected eluates were extracted three times with EtOAc (1:1; v/v), organic fractions were combined where appropriate, evaporated, and the residue was redissolved in 80% aqueous methanol (1 μL/20 mg initial fresh weight). Desulfoglucosinolates were prepared from freeze-dried root material, using DEAE Sephadex A-25 (Fluka, Buchs, Switzerland), following the protocol of Mikkelsen et al. (2003) with minor modifications. Secreted compounds were isolated from root culture liquid acidified with 0.1% trifluoroacetic acid using Discovery DSC-18 SPE cartridges (100 mg; Supelco). Compounds adsorbed by the resin were eluted with 1 mL methanol. The solvent was removed as above and the residues were redissolved in 200 μL 80% aqueous methanol.

All kinds of samples (20 μL) were subjected to HPLC on a Nucleosil C-18 column (EC 250/4, 120–5; Macherey & Nagel, Düren, Germany) using 0.1% trifluoroacetic acid as solvent A and 98% acetonitrile/0.1% trifluoroacetic acid as solvent B at a flow rate of 1 mL/min at 24°C (gradient of solvent A: 100% at 0, 94% at 3, 80% at 13, 76% at 20, 20% at 33, 0% at 34 min) and a Photodiode Array Detector 540 at 254 nm as part of the Bio-Tek System (Solvent Delivery System 522, Autosampler 565, Jet-Stream Plus, Degasy DG 1210, software CHROMA 2000; Bio-Tek, Neufahrn, Germany). For preparative HPLC, a Nucleosil C-18 SP 250/10 120 to 5 column and the respective part of the gradient were used under otherwise identical conditions. The metabolites of interest were quantified based on comparison of their peak areas with those obtained during HPLC analyses of known amounts either of respective purified compounds or of indole-3-carboxylic acid (Merck, Darmstadt, Germany; **14** and **15**) or of scopoletin (Roth, Karlsruhe, Germany; **3**).

RNA-Gel Blotting

cDNAs of *C4H* (At2g30490), *TSB1* (At5g54810), *CYP79B2* (At4g39950), and *PAL1* (At2g37040; Newman et al., 1994; Yamada et al., 2003), were obtained from the Arabidopsis Biological Resource Center (Columbus, OH; respective stock nos. 118J10, 126P17, U09943, and U10120). To obtain DNA probes for *ASA1* (At5g05730), *CCR2* (At1g80820), *CYP79B3* (At2g22330), *CYP81B1* (At4g31500), and *TSA* (At3g54640), fragments of the respective genes were amplified by PCR from Col-0 genomic DNA. The following primers were used (sense and antisense, respectively): *ASA1*, ATGTCTTCCTCTATGAACGTAGC and CTATTGAAGCTTCCGGAGAAACAG; *CCR2*, CAAAAGATAAAAGACTTAGGCTTGG and AAAACCATTGCTTCCATTATCG; *CYP79B3*, GAGTCATGATATGTTTCTTTCG and CCTTCTTATTAATCATCAAAAC; *CYP81B1*, AACCAGAGGATATAAAGATGGAC and CGTTAAAATGAGAACATAGTACTC; *TSA*, AAACAAAGATGGAAGAGCAAG and TTGAGATTTTGGGGATTGGAG. PCR products were cloned into pDrive vector (Qiagen; Hilden, Germany) and confirmed by sequencing. Single-stranded, ^{32}P-labeled probes were synthesized using the Random Primed DNA Labeling kit (Roche, Mannheim, Germany) and gel-purified DNA fragments after digestions with *Sal*I and *Not*I (*C4H* and *TSB1*) or *Sfi*I (*CYP79B2* and *PAL1*) or *Eco*RI for the pDrive-based constructs.

Arabidopsis roots were ground in liquid nitrogen, and the RNA was isolated using the RNA Isolation Reagent (RNAwiz; Ambion, Austin, TX). The RNA (20 μg) was separated by electrophoresis on a 1.3% (w/v) agarose gel, visualized under UV light, transferred to nylon membranes, hybridized with ^{32}P-labeled probes, and analyzed as described earlier (Logemann and Hahlbrock, 2002).

NMR Spectroscopy

NMR analyses were carried out on a Bruker Avance DRX 500 spectrometer (Bruker Biospin, Karlsruhe, Germany). ^{1}H NMR, ^{1}H-^{1}H COSY, HMBC, and HMQC experiments were recorded at 500.13 MHz in a 2.5-mm inverse-detection microprobe head or a 5-mm TXI CryoProbe employing standard Bruker pulse sequences. Tetramethylsilane was used as internal reference. The majority of the ^{13}C chemical shift values were obtained from HMBC and HMQC spectra. For the individual NMR spectra, see supplemental data.

MS and LC-MS

Chemical structures were determined by electrospray (ESI)-MS using a Hewlett-Packard (Avondale, PA) HP 1100 HPLC coupled to a Micromass Quattro II (Waters, Micromass, Manchester, UK) tandem quadrupole mass spectrometer (geometry quadrupole-hexapole-quadrupole) equipped with an ESI source. The capillary and cone voltages in ESI mode were 3.3 kV and 18 V, respectively. Nitrogen for nebulization was applied at 15 L/h, drying gas at 250 L/h and 250°C. Source and capillary were heated at 80°C and 250°C, respectively. The mass spectrometer was operated in conventional scanning mode using the first quadrupole. Negative-ion and positive-ion full-scan mass spectra were recorded from mass-to-charge ratio 90 to 450 (scanning time 1.5 s). For several compounds (**4** and **7**), atmospheric pressure chemical ionization was used as described by Hagemeier et al. (2001). Fixed precursor-ion (MS/MS) spectra (daughter-ion scan) were recorded by setting the first quadrupole to transmit the parent ion of interest and scanning the product ions obtained after collision of parent ions in the hexapole gas cell using the second quadrupole analyzer. Fixed product spectra (parent-ion scan) were recorded by setting the second quadrupole to transmit the daughter ion of interest. Argon was used for collision-induced dissociations at 1.5 × 10^{-3} millibar pressure and the collision energy was varied from 12 to 50 eV for fragmentation. Samples (approximately 5–10 μL) dissolved in methanol were injected into mobile phase (50:50 acetonitrile:water, flow of 50 μL/min) using a Rheodyne valve. High resolution ESI-MS were recorded at a resolution of

approximately 2,500. A solution of polyethylene glycol oligomers (average molecular mass, 300 D; Aldrich, St. Louis; approximately 1 mg/mL) in methanol:1 mM ammonium acetate (1:1) was mixed with the sample (1:1) and delivered into ESI source using a syringe pump (Harvard Apparatus, Matick, MA) at a flow rate of 7 μL/min. Scans were measured in full mass mode from 250 to 500 D at 5 s/scan in a continuum mode and the data were collected in 128 data point mode. The measured scans were internally calibrated using polyethylene glycol $[M + H]^+$, $[M + NH_4]^+$, and $[M + Na]^+$ ion masses. Separation was achieved on a reverse-phase column (5 μm C18 phase, 250- × 2.1-mm i.d., Supelco) equipped with a precolumn (Supelco) using a gradient of 0.1% aqueous formic acid (A) and acetonitrile (B): 0 to 6 min, 2% to 4% B; 6 to 13 min, 4% to 18% B; 13 to 17 min, 18% to 28% B; 17 to 22 min, 28% to 53% B; 22 to 24 min, 53% to 93% B; 24 to 29 min, hold of 93% B (flow rate 0.4 mL/min, column temperature 30°C, UV detection at 228 nm).

High resolution electron ionization mass spectra were recorded using a MasSpec mass spectrometer (Micromass). Ionization was achieved at 70 eV electron energy and samples were introduced using a direct insertion probe. Positive ions were detected at minimum 3,000 resolution and internally calibrated with perfluorokerosene.

For the individual mass spectra, see supplemental data.

ACKNOWLEDGMENTS

We thank Dr. Jianwen Tan for help with the purification of some of the identified compounds, Drs. Michael Reichelt and Nicole van Dam for a kind gift of desulfoglucosinolate standards, and Drs. William Martin, Elmar W. Weiler, and Imre E. Somssich for valuable comments on the manuscript.

Received December 13, 2004; revised February 21, 2005; accepted March 15, 2005; published May 27, 2005.

LITERATURE CITED

Bais HP, Park SW, Weir TL, Callaway RM, Vivanco JM (2004) How plants communicate using the underground information superhighway. Trends Plant Sci **9:** 26–32

Bednarek P, Franski R, Kerhoas L, Einhorn J, Wojtaszek P, Stobiecki M (2001) Profiling changes in metabolism of isoflavonoids and their conjugates in *Lupinus albus* treated with biotic elicitor. Phytochemistry **56:** 77–85

Bednarek P, Winter J, Hamberger B, Oldham NJ, Schneider B, Tan J, Hahlbrock K (2004) Induction of 3′-*O*-β-D-ribofuranosyl adenosine during compatible, but not during incompatible, interactions of *Arabidopsis thaliana* or *Lycopersicon esculentum* with *Pseudomonas syringae* pathovar tomato. Planta **218:** 668–672

Bell-Lelong DA, Cusumano JC, Meyer K, Chapple C (1997) Cinnamate-4-hydroxylase expression in Arabidopsis (regulation in response to development and the environment). Plant Physiol **113:** 729–738

Bennett RN, Mellon FA, Foidl N, Pratt JH, Dupont MS, Perkins L, Kroon PA (2003) Profiling glucosinolates and phenolics in vegetative and reproductive tissues of the multi-purpose trees *Moringa oleifera* L. (horseradish tree) and *Moringa stenopetala* L. J Agric Food Chem **51:** 3546–3553

Bloor SJ, Abrahams S (2002) The structure of the major anthocyanin in *Arabidopsis thaliana.* Phytochemistry **59:** 343–346

Boerjan W, Ralph J, Baucher M (2003) Lignin biosynthesis. Annu Rev Plant Biol **54:** 519–546

Brader G, Tas E, Palva ET (2001) Jasmonate-dependent induction of indole glucosinolates in Arabidopsis by culture filtrates of the nonspecific pathogen *Erwinia carotovora.* Plant Physiol **126:** 849–860

Bradfield CA, Bjeldanes LF (1987a) High-performance liquid-chromatographic analysis of anticarcinogenic indoles in *Brassica oleracea.* J Agric Food Chem **35:** 46–49

Bradfield CA, Bjeldanes LF (1987b) Dietary modification of xenobiotic metabolism: contribution of indolylic compounds present in *Brassica oleracea.* J Agric Food Chem **35:** 896–900

Brown PD, Tokuhisa JG, Reichelt M, Gershenson J (2003) Variation of glucosinolate accumulation among different organs and developmental stages of *Arabidopsis thaliana.* Phytochemistry **62:** 471–481

Chapple CCS, Vogt T, Ellis BE, Somerville CR (1992) An Arabidopsis mutant defective in the general phenylpropanoid pathway. Plant Cell **4:** 1413–1424

Chong J, Baltz R, Schmitt C, Beffa R, Fritig B, Saindrenan P (2002) Downregulation of a pathogen-responsive tobacco UDP-Glc:phenylpropanoid glucosyltransferase reduces scopoletin glucoside accumulation, enhances oxidative stress, and weakens virus resistance. Plant Cell **14:** 1093–1107

Conn LK, Browne LM, Tewari JP, Ayer WA (1994) Resistance to *Rhizoctonia solani* and presence of antimicrobial compounds in *Camaelia sativa* roots. J Plant Biochem Biotechnol **3:** 125–130

Dixon RA (2001) Natural products and plant disease resistance. Nature **411:** 843–847

Flores HE, Vivanco JM, Loyola-Vargas VM (1999) 'Radicle' biochemistry: the biology of root-specific metabolism. Trends Plant Sci **4:** 220–226

Glawischnig E, Hansen BG, Olsen CE, Halkier BA (2004) Camalexin is synthesized from indole-3-acetaldoxime, a key branching point between primary and secondary metabolism in Arabidopsis. Proc Natl Acad Sci USA **101:** 8245–8250

Glazebrook J (2001) Genes controlling expression of defense responses in Arabidopsis-2001 status. Curr Opin Plant Biol **4:** 301–308

Glazebrook J, Ausubel FM (1994) Isolation of phytoalexin-deficient mutants of *Arabidopsis thaliana* and characterization of their interactions with bacterial pathogens. Proc Natl Acad Sci USA **91:** 8955–8959

Glazebrook J, Zook M, Mert F, Kagan I, Rogers EE, Crute IR, Holub EB, Hammerschmidt R, Ausubel FM (1997) Phytoalexin-deficient mutants of Arabidopsis reveal that *PAD4* encodes a regulatory factor and that four *PAD* genes contribute to downy mildew resistance. Genetics **146:** 381–392

Głowniak K, Zgórka G, Kozyra M (1996) Solid-phase extraction and reversed-phase high-performance liquid chromatography of free phenolic acids in some *Echinacea* species. J Chromatogr A **730:** 25–29

Hagemeier J, Schneider B, Oldham NJ, Hahlbrock K (2001) Accumulation of soluble and wall-bound indolic metabolites in *Arabidopsis thaliana* leaves infected with virulent or avirulent *Pseudomonas syringae* pathovar tomato strains. Proc Natl Acad Sci USA **98:** 753–758

Hahlbrock K, Bednarek P, Ciolkowski I, Hamberger B, Heise A, Liedgens H, Logemann E, Nürnberger T, Schmelzer E, Somssich IE, et al (2003) Non-self recognition, transcriptional reprogramming, and secondary metabolite accumulation during plant/pathogen interactions. Proc Natl Acad Sci USA **100:** 14569–14576

Harborne JB (1999) The comparative biochemistry of phytoalexin induction in plants. Biochem Syst Ecol **27:** 335–367

Hase T, Koreeda M, Hasegawa K (1983) A growth inhibitor, 2-thioxothiazolidine-4-carboxylic acid from Sakurajima radish seedlings. Phytochemistry **22:** 1275–1276

Hemm MR, Rider SD, Ogas J, Murry DJ, Chapple C (2004) Light induces phenylpropanoid metabolism in Arabidopsis roots. Plant J **38:** 765–778

Hemm MR, Ruegger MO, Chapple C (2003) The Arabidopsis *ref2* mutant is defective in the gene encoding CYP83A1 and shows both phenylpropanoid and glucosinolate phenotypes. Plant Cell **15:** 179–194

Hogge LR, Reed DW, Underhill EW, Haughn GW (1988) HPLC separation of glucosinolates from leaves and seeds of *Arabidopsis thaliana* and their identification using thermospray liquid chromatography/mass spectrometry. J Chromatogr Sci **26:** 551–556

Jones P, Messner B, Nakajima JI, Schäffner AR, Saito K (2003) UGT73C6 and UGT78D1: glycosyltransferases involved in flavonol glycoside biosynthesis in *Arabidopsis thaliana.* J Biol Chem **278:** 43910–43918

Kloek AP, Verbsky ML, Sharma SB, Schoelz JE, Vogel J, Klessig DF, Kunkel BN (2001) Resistance to *Pseudomonas syringae* conferred by an *Arabidopsis thaliana* coronatine-insensitive (coi1) mutation occurs through two distinct mechanisms. Plant J **26:** 509–522

Kreuzaler F, Hahlbrock K (1973) Flavonoid glycosides from illuminated cell suspension cultures of *Petroselinum hortense.* Phytochemistry **12:** 1149–1152

Latxague L, Gardrat C, Coustille JL, Viaud MC, Rollin P (1991) Identification of enzymatic degradation products from synthesized glucobrassicin by gas chromatography-mass spectrometry. J Chromatogr A **586:** 166–170

Lauvergeat V, Lacomme C, Lacombe E, Lasserre E, Roby D, Grima-Pettenati J (2001) Two cinnamoyl-CoA reductase (CCR) genes from *Arabidopsis thaliana* are differentially expressed during development

and in response to infection with pathogenic bacteria. Phytochemistry **57:** 1187–1195

Li J, Ou-Lee TM, Raba R, Amundson RG, Last RL (1993) Arabidopsis flavonoid mutants are hypersensitive to UV-B irradiation. Plant Cell **5:** 171–179

Ljung K, Hull AK, Kowalczyk M, Marchant A, Celenza J, Cohen JD, Sandberg G (2002) Biosynthesis, conjugation, catabolism and homeostasis of indole-3-acetic acid in *Arabidopsis thaliana.* Plant Mol Biol **50:** 309–332

Logemann E, Hahlbrock K (2002) Crosstalk among stress responses in plants: Pathogen defense overrides UV protection through an inversely regulated ACE/ACE type of light-responsive gene promoter unit. Proc Natl Acad Sci USA **99:** 2428–2432

Ludwig-Müller J, Pieper K, Ruppel M, Cohen JD, Epstein E, Kiddle G, Bennett R (1999) Indole glucosinolate and auxin biosynthesis in *Arabidopsis thaliana* (L.) Heynh. glucosinolate mutants and the development of clubroot disease. Planta **208:** 409–419

Mansfield JW (2000) Antimicrobial compounds and resistance. The role of phytoalexins and phytoanticipins. *In* A Slusarenko, RSS Fraser, LC van Loon, eds, Mechanisms of Resistance to Plant Diseases. Kluwer Academic Publishers, Dordrecht, The Netherlands, pp 325–370

Marquez LA, Dunford HB (1995) Transient and steady-state kinetics of the oxidation of scopoletin by horseradish peroxidase compounds I, II and III in the presence of NADH. Eur J Biochem **233:** 364–371

Mikkelsen MD, Petersen BL, Glawischnig E, Jensen AB, Andreasson E, Halkier BA (2003) Modulation of CYP79 genes and glucosinolate profiles in Arabidopsis by defense signaling pathways. Plant Physiol **131:** 298–308

Müller E, Weiler EW (2000) Indolic constituents and indole-3-acetic acid biosynthesis in the wild-type and a tryptophan auxotroph mutant of *Arabidopsis thaliana.* Planta **211:** 855–863

Narasimhan K, Basheer C, Bajic VB, Swarup S (2003) Enhancement of plant-microbe interactions using a rhizosphere metabolomics-driven approach and its application in the removal of polychlorinated biphenyls. Plant Physiol **132:** 146–153

Newman T, de Bruijn FJ, Green P, Keegstra K, Kende H, McIntosh L, Ohlrogge J, Raikhel N, Somerville S, Thomashow M, et al (1994) Genes galore: a summary of methods for accessing results from large-scale partial sequencing of anonymous Arabidopsis cDNA clones. Plant Physiol **106:** 1241–1255

Nomoto M, Tamura S (1970) Isolation and identification of indole derivatives in clubroots of Chinese cabbage. Agric Biol Chem **34:** 1590–1592

Pedras MSC, Chumala PB, Suchy M (2003) Phytoalexins from *Thlaspi arvense,* a wild crucifer resistant to virulent *Leptosphaeria maculans*: structures, syntheses and antifungal activity. Phytochemistry **64:** 949–956

Peer WA, Brown DE, Tague BW, Muday GK, Taiz L, Murphy AS (2001) Flavonoid accumulation patterns of transparent testa mutants of Arabidopsis. Plant Physiol **126:** 536–548

Petersen BL, Chen S, Hansen CH, Olsen CE, Halkier BA (2002) Composition and content of glucosinolates in developing *Arabidopsis thaliana.* Planta **214:** 562–571

Radwanski ER, Last RL (1995) Tryptophan biosynthesis and metabolism: biochemical and molecular genetics. Plant Cell **7:** 921–934

Reintanz B, Lehnen M, Reichelt M, Gershenzon J, Kowalczyk M, Sandberg G, Godde M, Uhl R, Palme K (2001) Bus, a bushy Arabidopsis CYP79F1 knockout mutant with abolished synthesis of short-chain aliphatic glucosinolates. Plant Cell **13:** 351–367

Rogers EE, Glazebrook J, Ausubel FN (1996) Mode of action of the *Arabidopsis thaliana* phytoalexin camalexin and its role in Arabidopsis-pathogen interactions. Mol Plant Microbe Interact **9:** 748–757

Staswick PE, Yuen GY, Lehman CC (1998) Jasmonate signaling mutants of Arabidopsis are susceptible to the soil fungus *Pythium irregulare.* Plant J **15:** 747–754

Tan J, Bednarek P, Liu J, Schneider B, Svatos A, Hahlbrock K (2004) Universally occurring phenylpropanoid and species-specific indolic metabolites in infected and uninfected *Arabidopsis thaliana* roots and leaves. Phytochemistry **65:** 691–699

Thies W (1979) Detection and utilization of a glucosinolate sulfohydrolase in the edible snail *Helix pomatia.* Naturwissenschaften **66:** 364–365

Thomma BPHJ, Nelissen I, Eggermont K, Broekaert WF (1999) Deficiency in phytoalexin production causes enhanced susceptibility of *Arabidopsis thaliana* to the fungus *Alternaria brassicicola.* Plant J **19:** 163–171

Tsuji J, Jackson EP, Gage DA, Hammerschmidt R, Sommerville SC (1992) Phytoalexin accumulation in *Arabidopsis thaliana* during the hypersensitive response to *Pseudomonas syringae* pv *syringae.* Plant Physiol **98:** 1304–1309

VanEtten HD, Mansfield JW, Bailey JA, Farmer EE (1994) Two classes of plant antibiotics: phytoalexins versus ''phytoanticipins''. Plant Cell **6:** 1191–1192

van West P, Appiah AA, Gow NAR (2003) Advances in research on oomycete root pathogens. Physiol Mol Plant Pathol **62:** 99–113

von Roepenack-Lahaye E, Degenkolb T, Zerjeski M, Franz M, Roth U, Wessjohann L, Schmidt J, Scheel D, Clemens S (2004) Profiling of Arabidopsis secondary metabolites by capillary liquid chromatography coupled to electrospray ionization quadrupole time-of-flight mass spectrometry. Plant Physiol **134:** 548–559

Veit M, Pauli GF (1999) Major flavonoids from *Arabidopsis thaliana* leaves. J Nat Prod **62:** 1301–1303

Vijayan P, Shockey J, Levesque CA, Cook RJ, Browse J (1998) A role for jasmonate in pathogen defense of *Arabidopsis.* Proc Natl Acad Sci USA **95:** 7209–7214

Wakabayashi K, Nagao M, Tahira T, Yamaizumi Z, Katayama M, Marumo S, Sugimura T (1986) 4-Methoxyindole derivatives as nitrosable precursors of mutagens in Chinese cabbage. Mutagenesis **1:** 423–426

Walker TS, Bais HP, Grotewold E, Vivanco JM (2003a) Root exudation and rhizosphere biology. Plant Physiol **132:** 44–51

Walker TS, Bais HP, Halligan KM, Stermitz FR, Vivanco JM (2003b) Metabolic profiling of root exudates of *Arabidopsis thaliana.* J Agric Food Chem **51:** 2548–2554

Wanner LA, Li GQ, Ware D, Somssich IE, Davis KR (1995) The phenylalanine ammonia-lyase gene family in *Arabidopsis thaliana.* Plant Mol Biol **27:** 327–338

Whetten R, Sederoff R (1995) Lignin biosynthesis. Plant Cell **7:** 1001–1013

Wittstock U, Halkier BA (2002) Glucosinolate research in the Arabidopsis era. Trends Plant Sci **7:** 263–270

Yamada K, Lim J, Dale JM, Chen H, Shinn P, Palm CJ, Southwick AM, Wu HC, Kim C, Nguyen M, et al (2003) Empirical analysis of transcriptional activity the Arabidopsis genome. Science **302:** 842–846

Zhao J, Last RL (1996) Coordinate regulation of the tryptophan biosynthetic pathway and indolic phytoalexin accumulation in Arabidopsis. Plant Cell **8:** 2235–2244

Zhou N, Tootle TL, Glazebrook J (1999) Arabidopsis *PAD3,* a gene required for camalexin biosynthesis, encodes a putative cytochrome P450 monooxygenase. Plant Cell **11:** 2419–2428

Zook M, Hammerschmidt R (1997) Origin of the thiazole ring of camalexin, a phytoalexin from *Arabidopsis thaliana.* Plant Physiol **113:** 463–468

Zubieta C, Ross JR, Koscheski P, Yang Y, Pichersky E, Noel JP (2003) Structural basis for substrate recognition in the salicylic acid carboxyl methyltransferase family. Plant Cell **15:** 1704–1716